

УДК 538.9
doi: 10.18101/2306-2363-2016-2-3-26-34

© N. Tuvjargal, D. Baatarkhuu, T. Ochirkhuyag,
J. Davaasambu, P. Zuzaan

SPECTROSCOPIC STUDY OF GAMMA-IRRADIATED MONGOLIAN NATURAL QUARTZ

In this work we performed a spectroscopic characterization of natural quartz samples from Mongolia. These materials were examined by X-ray powder diffraction (XRD), UV-visible spectroscopy (UV-vis) and electron paramagnetic resonance (EPR). Samples were used in this study in as-received, gamma-irradiated and heat-treated conditions. The color formation in natural quartz through this procedure is explained based on XRD, EPR, and UV-VIS studies of gamma irradiated and heat-treated samples. Smoky quartz shows absorption bands in the visible region and a strong EPR signal. After heat-treatment it shows absorption bands in the near UV region with extensions into the visible region and a weak EPR signal.

Keywords: quartz, gamma-ray, heat treatment, spectroscopy, electron paramagnetic resonance, UV-visible spectroscopy, powder diffraction

Н. Тувжаргал, Д. Батаархуу, Т. Очиркхуаг,
Ж. Даваасамбу, П. Зузаан

СПЕКТРОСКОПИЧЕСКИЕ ИССЛЕДОВАНИЯ ГАММА- ОБЛУЧЕННЫХ МОНГОЛЬСКИХ ПРИРОДНЫХ КВАРЦОВ

В работе представлены спектроскопические характеристики природных образцов кварца из Монголии. Эти материалы были исследованы с помощью рентгеновской дифракции на порошковом образце (XRD), УФ-видимой спектроскопии (UV-vis) и электронного парамагнитного резонанса (ЭПР). Образцы использованные в этом исследовании были, в исходном виде, гамма-облученном и термообработанном состояниях. Формирование цвета в природном кварце в результате этой процедуры можно объяснить основываясь на РСА, ЭПР и UV-VIS исследованиях гамма-облученных и термически обработанных образцов. Дымчатый кварц показывает полосы поглощения в видимой области спектра, а также сильный сигнал ЭПР. После термической обработки он показывает полосы поглощения в ближней UV области, а также слабый сигнал ЭПР.

Ключевые слова: кварц, гамма облучения, термическая обработка, спектроскопия, электронный парамагнитный резонанс, УФ-видимая спектроскопия, рентгеновская дифракция

Quartz is one of the most abundant minerals in earth's crust. It is well established that this material show a SiO₄ tetrahedron as its basic structural unit. It

belongs to a class of materials known as tectosilicates where the oxygen atoms at the corners of each SiO_4 tetrahedron are shared with adjacent tetrahedra. Quartz has been used in many fields, including dating, dosimeter, and electronics. It is also worth highlighting the use of this material in jewelry [1, 2].

It has always been in interests of scientists and researchers to turn semi-precious and precious stones into any color and shape. Very attractive property of stones is that their colors changed into different colors by not only adding additional elements into them but also putting them under gamma ray radiation [3, 4]. It is important to explain how this process could be possible and how it works. Colorless quartz becomes smoky or dark smoky when exposed to gamma rays. Smoky quartz may become brownish, or colorless after heat-treatment. Natural, colorless quartz is routinely colored by irradiation with gamma rays and heat-treatment for jewelry production.

Its atomic structure is particularly simple, which helps in the study of point defects. Attention has been specifically focused on structures, electronic properties and generation mechanisms of defects in this material. In general, point defects can be usefully related to modifications of some macroscopic properties, as the appearance of optical absorption and of Electron Paramagnetic Resonance (EPR) signals. In many cases the defect formation depends on the manufacturing procedure of the material and on later treatments [5].

We report experimental studies of the effects of gamma radiation induced in natural quartz. The main target is the spectroscopic characterization of induced point defects and the identification of their formation mechanisms. To this purpose we use EPR spectroscopy and obtain complementary information from optical absorption measurements. This multi-technique approach proves to be very useful to evidence when distinct spectroscopic features can be attributed to the same defect and when correlations point out the possible existence of defect conversion.

Gamma ray induced point defect in quartz

In general, a point defect can be visualized as a local distortion of the atomic structure caused by a bond rupture, an over or under coordinated atom, the presence of an impurity atom (homo or heterovalent substitution, interstitial,...), etc. [6]. These defects are usually indicated as *intrinsic* when they are due to irregular arrangements of the crystal atoms (Si and O for SiO_2), and *extrinsic* when they are related to impurities (atoms differing from Si or O).

A further general classification of the point defects, useful in the following discussion, can be made on the basis of their electronic configuration: those having unpaired electrons constitute *paramagnetic* defects, and the others are the *diamagnetic* defects. Both typologies could in principle be characterized by optical activities as absorption and emission bands. Instead, only the paramagnetic defects have a further feature since they are responsible for a non-zero magnetic moment, having unpaired electrons, and are responsible for the magnetic resonance absorption.

Examples of the point defects are: the *vacancy* (an atom is removed from its "reticular" position), the *interstitial* (an atom is in a non-reticular position) and the *valence defect* (a bond Si-O is broken). In particular, among the intrinsic defects in

silica we found the neutral oxygen vacancy: $\text{O}\equiv\text{Si}-\text{Si}\equiv\text{O}$, the peroxy bridge: $\text{O}\equiv\text{Si}-\text{O}-\text{O}-\text{Si}\equiv\text{O}$, the non-bridging oxygen: $\text{O}\equiv\text{Si}-\text{O}^\cdot$ (NBOHC), the tricoordinated silicon: $\text{O}\equiv\text{Si}^\cdot$ (usually named E' center), the twofold coordinated silicon: $\text{O}=\text{Si}^{\cdot\cdot}$. Some of these defects are pictorially reported in fig. 1. It is worth to note that these defects may present several charge states due to electron or hole trapping [4, 7].

Electronic states (ground and excited) of a point defect may have energy separation lower than the energy-gap (~ 8 eV) of the silica matrix. For instance, the broken bond defects, like $\text{O}\equiv\text{Si}-\text{O}^\cdot$ or $\text{O}\equiv\text{Si}^\cdot$, are related to the (anti-bonding) localized states that should be found between the valence and the conduction band [4]. As a consequence, the transitions among electronic states of the defect, induced by the electromagnetic field, give rise to absorption and emission bands with energy spanning from below ~ 2.0 eV, in the visible range, up to ~ 8 eV, in the vacuum UV (VUV) region, which explains the loss of transparency of the material. Also, the defects may trap charge, electron or hole, so they influence the insulation properties of silica. Finally, in the case of paramagnetic defects a redistribution of the electronic levels is introduced by a very small energy separation (~ 10 meV) and related to the presence of a magnetic field, so varying the magnetic properties of the material.

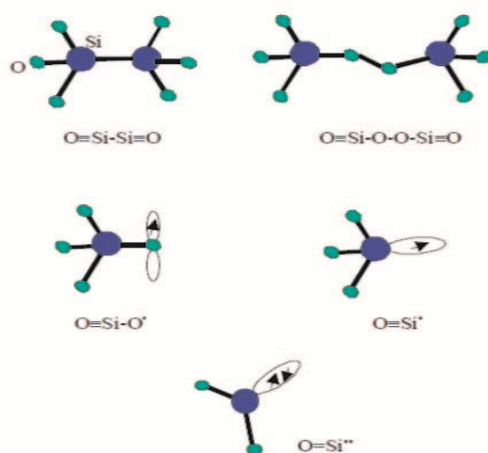


Fig. 1. Fragments of amorphous silica pictorially representing various point defects. The electrons spins, inserted in pictorial orbitals are indicated by arrows

Various optical absorption and emission bands as well as EPR structures, in the case of paramagnetic defects, have been detected. From them, energy level diagrams for the defects have been derived together with, in the case of the EPR, information on the electronic orbital and on their atomic environment. However, it is very difficult to correlate such information to a particular structural model of the defect and only in few cases, following ad-hoc experiments, as e.g. for the $\text{O}\equiv\text{Si}-\text{O}^\cdot$, $\text{O}\equiv\text{Si}^\cdot$ centers, that were observed in ^{29}Si and ^{17}O isotopic enriched samples [8], a successful determination has been done.

A particularly useful technique in the investigation of the mechanisms of defect generation is the irradiation of quartz with beam of particles (electrons, neutrons, ions, etc.) or ionizing radiation (UV, X, γ , etc.) [4, 7]. Two main mechanisms are distinguished:

- the *knock-on* processes, in which atomic displacements are caused by the direct transfer of the projectile kinetic energy;
- the *radiolysis* processes, in which atomic motion or bond ruptures are caused through ionization or electron excitation.

In the knock-on processes the projectile particles of the incident beam interact directly with the atoms of the material causing displacements (for example, vacancy-interstitial Frenkel pair) or site distortions. Two kinds of knock-on processes are generally considered: the elastic, that conserves the total kinetic energy, and the inelastic, in which some of the projectile kinetic energy is lost in electronic transitions (excitation, ionization,...) or nuclear reactions [4]. In order to create defects by displacements, it is necessary that the projectile gives sufficient energy to the target atom to break its bonds and to prevent that the knocked-on atom is recaptured from its neighboring atoms. The value of this energy for a given atom in the matrix is called displacement energy T_d , and it has been estimated that, in SiO_2 , $T_d^{\text{O}} \cong 10$ eV and $T_d^{\text{Si}} \cong 20$ eV, for O and Si displacements, respectively, assuming an Si-O bond energy of ~ 5 eV [9].

The radiolysis processes (electronic excitation, ionizations and bond rupture) have been found to be predominant in electron and γ irradiation as they overcome the efficiency of the knock-on processes by at least an order of magnitude [3, 4]. On the other hand, only radiolysis processes are possible when sub-band gap photons like UV are employed. It is worth to note that in the case of energetic irradiation particles a cascade of radiolysis processes could be induced since several electron-hole pairs are created by the scattered projectile [4]. Among the various irradiation damage sources the γ rays are very interesting. They can act through photoelectric effect, Compton effect and pair production (electron-positron) [10] and give rise to primary electrons and a cascade of scattered energetic electrons and photons. Depending on the γ photon energy one of the above processes prevails [11].

Thermal annealing is another external treatment frequently used for the investigation of point defects. In fact, many varieties of radiation-induced defects can be destroyed on increasing the temperature, as for the case of the E' centers [8]. In general, by warming an irradiated material it is possible to individuate the temperature at which a given defect is destroyed. By this way useful information related to the defect structure, as for example the strength of the molecular-bonds and the depth of the defect potential well, can be obtained. Also, the study of thermal behavior can be used to evidence the existence of correlations. For example, it is possible to establish if macroscopic properties, like optical absorption bands or EPR signals, are related to one defect when they follows the same kinetics under the action of a given thermal treatment.

Experiments

In this work we used natural quartz from Mongolia. Samples were used in this study in natural, gamma irradiated and heat-treated conditions. It is important mentioning that the natural quartz samples showed colorless. Colorless quartz becomes smoky or dark smoky when exposed to gamma rays. Smoky quartz may be come brownish, or colorless after heat-treatment. The gamma-irradiation step was performed in Microtron MT-22 (Nuclear physics research center, National University of Mongolia) at 0-22 MeB continuous radiation energy, 9 μ A electron current and $\Phi_{\gamma}=(7.2 \cdot 10^{11}-1.2 \cdot 10^{11})\gamma/\text{sm}^2 \cdot \text{sec} \cdot \mu\text{A}$ radiation flux density.

The heat treatment step of quartz samples was performed in air, using a T 6200 (Heraeus) furnace and cooling/heating rates of 10°C/min. Samples were kept at 200°C for 24 h.

XRD was performed in a Philips-PANalytical PW1800 diffractometer, using $\text{CuK}\alpha$ radiation and operating at 40 kV and 30 mA.

UV-vis spectra were taken in the spectral range from 200 to 800 nm, using a Shimadzu UV-2401PC spectrometer and a resolution of 0.1 nm. EPR spectra were taken in $\Delta H=200$ G, $H_r=1200$ G, $\tau=0.3$ sec, $\Delta t=30$ sec using SEPR2 EPR spectrometer. The EPR spectra were taken at room temperature and recorded as the first derivative of the absorption curve. A coal reference sample was used to determine paramagnetic defect concentration in as-received, gamma-irradiated and heat-treated Quartz. These tests were performed for samples in crystalline and powdered conditions.

Results and discussion

Samples were used in this study in as-received, gamma irradiated and heat-treated conditions. Fig.1 shows colorless quartz becomes smoky or dark smoky when irradiated to gamma rays. Smoky quartz may become brownish, or colorless after heat-treatment.

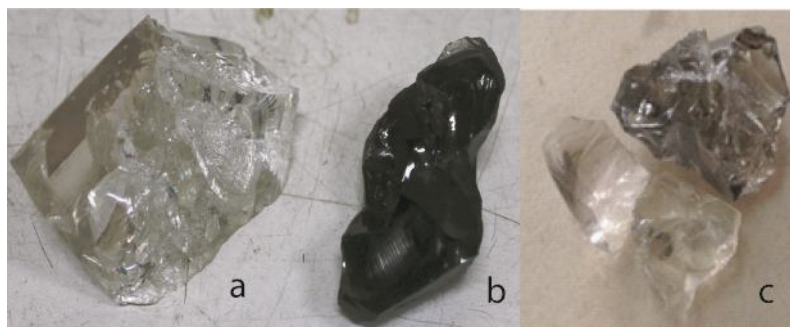


Fig. 1. Sample of (a) natural, (b) gamma irradiated and (c) heat-treated Quartz

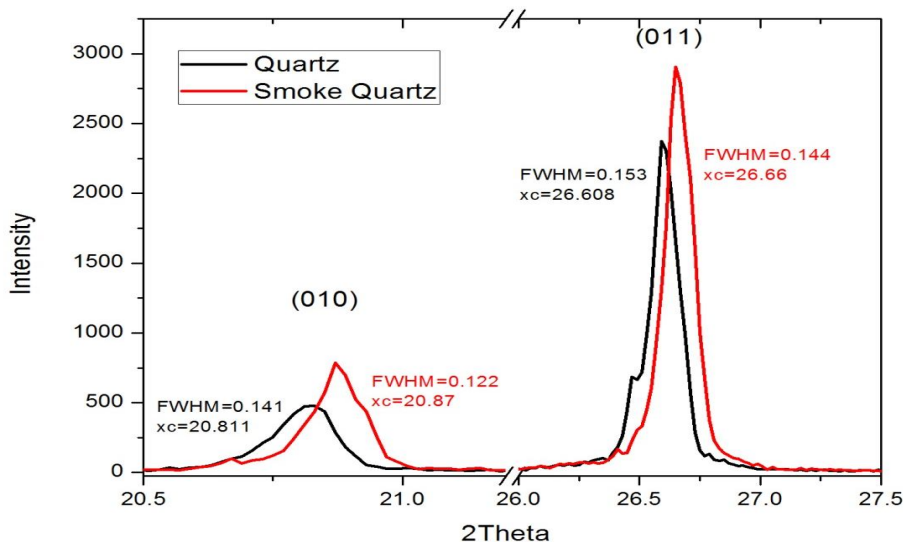


Fig. 2. XRD spectra of (010) and (011) crystallographic direction in natural and gamma irradiated Quartz

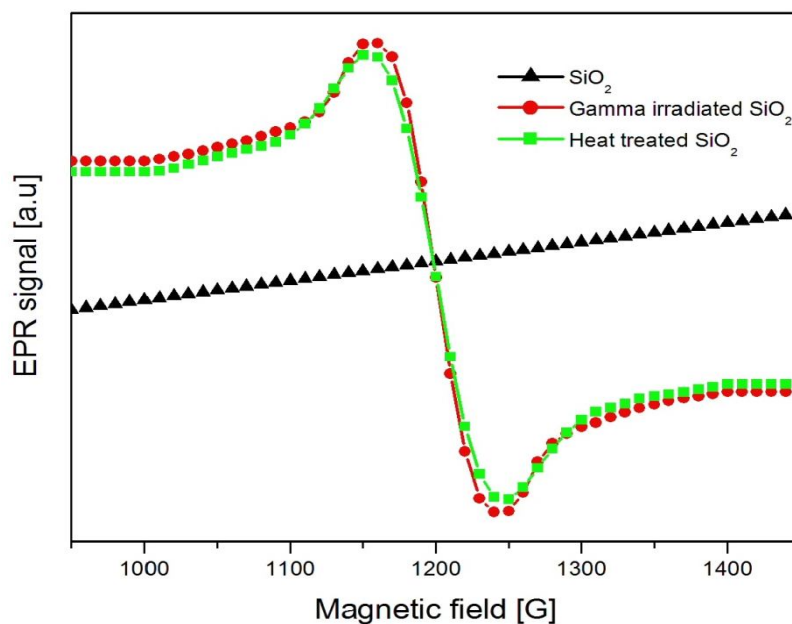


Fig. 3. EPR spectra of powdered in natural, gamma irradiated and heat-treated quartz samples

We observed that natural and gamma irradiated quartz showed XRD diffraction intensity variation in fig. 2 [12]. This observed diffraction peaks shift may be related to atomic displacement in quartz is given by the following equation,

$$I \approx F^2; \quad F_{hkl} = \sum_{i=1}^n f_i T \exp[2\pi i (hx_i + ky_i + lz_i)]. \quad (1)$$

Fig. 3 shows powder EPR spectra of natural, gamma irradiated and heat-treated quartz samples. Most of the resonance lines observed in these spectra could be associated to gamma radiation induced paramagnetic center of Quartz. Gamma ray induced paramagnetic center concentrations in the samples are determined by the use of integral intensities of their EPR spectra and the spectra of the reference with the known amounts of paramagnetic centers. Paramagnetic center concentrations (N) in the samples are determined as the value which is proportional to the area under the absorption curves and the integral intensity (I) [14]. Integral intensities (I) of the absorption line were obtained by integration of this curve. Double integration of the first-derivative EPR spectra gives us the value of integral intensity (I). To obtain paramagnetic concentration the EPR lines of the tested samples and the references are measured. In our EPR studies of coal references were used [13]. Paramagnetic centers concentrations were obtained for gamma irradiated and heat treated quartz. Gamma irradiated sample is paramagnetic centers concentrations has been $6.6 \cdot 10^{18}$ spin/g. Heat treated sample is paramagnetic centers concentrations has been $5.9 \cdot 10^{18}$ spin/g.

Paramagnetic centers concentration is reduced after heat treatment in gamma irradiated quartz.

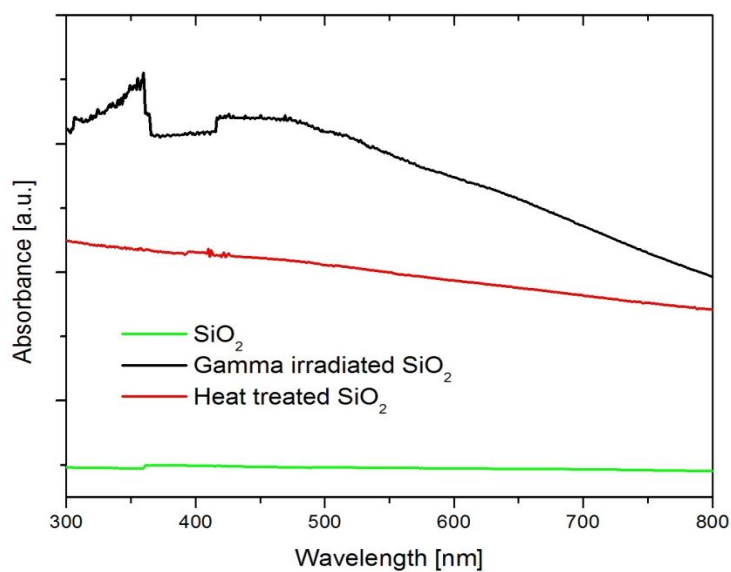


Fig. 4. UV-vis spectra of natural, gamma irradiated and heat-treated quartz samples

Fig. 4 shows UV-vis absorption spectra of natural, gamma irradiated and heat-treated quartz samples. We observed the presence of a broad absorption band at about 450 nm in the spectrum of the gamma-irradiated sample. In addition, one

notices the presence of an intense absorption in the near UV region, with extensions into the visible region. The combination of these bands gives rise to a dark black colored material. The heat-treatment of this material led to the complete bleaching of its color. The UV-vis spectrum of the heat-treated sample exhibited an almost constant absorption over the visible region.

Conclusions

The color formation in natural quartz through this procedure is explained based on XRD, EPR, and UV-VIS studies of natural, gamma irradiated and heat-treated samples. XRD spectra revealed diffraction peaks shift in some crystallographic direction. This peaks shift may be related to the atomic displacement in quartz.

We observed the changes in the EPR spectra and UV-vis of these samples as a function of the condition they were analyzed (natural, gamma-irradiated and heat-treated). Smoky quartz showed absorption bands in the visible region and a strong EPR signal. After heat-treatment it showed absorption bands in the near UV region with extensions into the visible region and a weak EPR signal. Therefore, gamma radiation induced color change in quartz which could be related to paramagnetic defects.

Acknowledgement

The work was supported by MMECS and FST under project SST_018/2015.

Reference

1. Klein C. The Manual of Mineral Science, twenty third ed. - NY: John Wiley & Sons. - 2002. - 704 p.
2. MacKeever S. W. S. Thermoluminescence in quartz and silica // *Radiat. Protect. Dosim.* - 2006. - V. 119. - P. 168-171.
3. Defects and disorder in crystalline and amorphous solids // Ed. Catlow R. - Kluwer Academic Publishers. - 1994. - 510 p.
4. Structure and imperfections in amorphous and crystalline silicon dioxide // Eds. Devine R. A. B, Duraud J. P., Dooryhée E. - NY: John Wiley and Sons. - 2000. - 349 p.
5. Agnello S., Boscaino R., Cannas M., Gelardi F. M. and Leone M. Gamma-ray-induced bleaching in silica: Conversion from optical to paramagnetic defects // *Physical Review B.* - 2000. - V. 61. - P. 1946-1951.
6. Kittel C. Introduction to Solid State Physics. - NY: John Wiley & Sons. - 1971. - 680 p.
7. de Novion C. H and Barbu A. In Materials under irradiation. Eds. Dunlop A. et al. // *J. Trans Tech Publications Ltd.* - 1993. - 277 p.
8. Griscom D. L. Optical properties and structure of defects in silica glass // *J. Ceramic Society of Japan.* - 1991. - V. 99. - P. 899-916.
9. Gupta R. P. Electronic structure of crystalline and amorphous silicon dioxide // *Phys. Rev. B.* - 1985. - V. 32. - P. 8278-8285.
10. Balanzat E. and Bouffard S. In Materials under irradiation. Eds. Dunlop A. et al. // *J. Trans Tech Publications Ltd.* - 1993. - P. 7-21.

11. Hubbell J. H. Photon cross section compilation activity in the U.S. in the range // J. de Physique. - 1971. - V. 32. - P. 14-23.
12. Tuvjargal N., Baatarkhuu D. et al. Scientific Transaction of the National University of Mongolia. Physics. - 2015. - V. 20. - P. 438-423.
13. Tuvjargal N., Baatarkhuu D. et al. Scientific Transaction of the National University of Mongolia. Physics. - 2016. - V. 22. - P. 449-453.
14. Weil J. A, Bolton J. R. Electron Paramagnetic Resonance: Elementary Theory and Practical Applications. - 2nd Edition. NY: John Wiley & Sons. - 2007. - 688 p.

Tuvjargal N., Department of Physics, School of Sciences and Arts, National University of Mongolia, Ulaanbaatar, Mongolia, E-mail: tuvjargal@num.edu.mn, tuvjargal@gmail.com

Baatarkhuu D., Nuclear Physics Research Center, National University of Mongolia, Ulaanbaatar, Mongolia

Ochirkhuyag T., Department of Physics, School of Sciences and Arts, National University of Mongolia, Ulaanbaatar, Mongolia

Davaasambuu J., Department of Physics, School of Sciences and Arts, National University of Mongolia, Ulaanbaatar, Mongolia

Zuzaan P., Department of Physics, School of Sciences and Arts, National University of Mongolia, Ulaanbaatar, Mongolia

Тувжаргал Н., Отделение физики, школа наук и искусств, Национальный университет Монголии, Монголия, Улан-Батор, E-mail: tuvjargal@num.edu.mn, tuvjargal@gmail.com

Батаархуу Д., Научно-исследовательский центр ядерной физики, Национальный университет Монголии, Монголия, Улан-Батор

Очиркхуаг Т., Отделение физики, школа наук и искусств, Национальный университет Монголии, Монголия, Улан-Батор

Даваасамбу Ж., Отделение физики, школа наук и искусств, Национальный университет Монголии, Монголия, Улан-Батор

Зузаан П., Отделение физики, школа наук и искусств, Национальный университет Монголии, Монголия, Улан-Батор